J. Fluid Mech. (1990), *vol.* 211, *pp.* 629–651
Printed in Great Britain

Knotted vortex filaments in an ideal fluid

By J. P. KEENER
Department of Mathematics, University of Utah, Salt Lake City, UT 84112, USA

(Received 27 March 1989 and in revised form 1 August 1989)

Knotted closed-curve solutions of the equation of self-induced vortex motion are studied. It is shown that there are invariant torus knots which translate and rotate as rigid bodies. The general motion of 'small-amplitude' torus knots and iterated (cabled) torus knots is described and found to be almost periodic in time, and for some, but not all, initial data, the topology of the knot is shown to be invariant.

1. Introduction

The equation of self-induced motion of a vortex filament in an ideal fluid is known to have a rich solution structure. It is known that this equation can be re-expressed in the form of the nonlinear Schrödinger equation to which the inverse scattering theory can be applied. As a result, for an infinitely long filament there are solitary pulse solutions, which correspond to one wrap of a helix around a long cylinder (Hasimoto 1972; Lamb 1981).

The solitary pulse is an example of a translation-invariant solution, but there are others. In fact, the shape of all translationally invariant closed-curve solutions has been found and can be expressed in terms of elliptic functions (Kida 1981). These solutions are of further interest from a geometrical and topological point of view because they are closed knotted curves in space.

The purpose of this paper is to examine the dynamic behaviour of closed knotted vortex filaments. We shall examine the translationally invariant knotted filaments as well as those which are not invariant. Specifically we shall study the dynamic behaviour of small-amplitude torus knots and certain iterated (cabled) torus knots.

The knotted solutions found here are constructed using regular perturbation arguments, and rigorous proofs of their existence can be given using the implicit function theorem. The key insight to using a perturbation method is to realize that a knotted curve can bifurcate from a circular curve if the solution of the underlying linear operator has the correct behaviour. For example, a trefoil knot can be viewed as a curve on a torus with winding number 3/2 (three wraps around the small radius of the torus for two wraps around the large radius). As the small radius of the torus is allowed to go to zero, the trefoil knot becomes a twisted multiple cover of a circle. Since a circle has constant curvature and zero torsion, bifurcation of a trefoil knot from a circle occurs if the deviation of the curvature from a constant and the torsion oscillate sinusoidally three times as the circle is traversed twice. Once this structure is understood, the construction of knots follows from standard perturbation arguments.

The invariant knots have been found completely and exactly (Kida 1981) by taking advantage of the special nature of the governing equations. The emphasis in this paper is on perturbation methods, which allows the study of equations of motion which do not have such a nice structure. Of course, being based on small parameter expansions, the method used here cannot find large-amplitude solutions.

The outline of this paper is as follows. In the next section we discuss the equation of motion under consideration, specifically the equation describing the motion of a vortex filament in an ideal fluid. We show some calculations that allow us to study the evolution of the curvature and torsion without reference to the extrinsic coordinate description of the filament, and reformulate the Frenet–Serret equations into a form that is relatively easy to study. In §3, we show how closed knotted curves in space can be found as solutions of the Frenet–Serret equations using perturbation methods. In §4 we show that the model equations have some special solutions, namely invariant torus knots that move in space as rigid bodies. These invariant solutions have been found previously using a different formulation of the problem (Kida 1981). In § 5 we study the general evolution of torus knots, and show the sense in which this motion can be viewed as a superposition of two of the simpler invariant knots as building blocks. It is also shown that the topology of these torus knots is invariant as a function of time. Finally, in §6, we study the dynamics of the simplest iterated torus knots, showing that their motion can be viewed as a superposition of four invariant torus knots. That is, the simple invariant torus knots behave like 'solitons' which can be superposed to construct knots with more complicated topology. For these knotted curves, conditions can be prescribed so that the topology is invariant, but there are also initial configurations for which there are self-intersections of the curve, changing its topology.

Numerical simulations of the knotted solutions described here have been done and are displayed graphically on a VHS format video tape, available on loan from the author for short periods of time.

2. The equations of motion

A curve R in three-dimensional space can be described in terms of its tangent, normal, and binormal vectors, $\boldsymbol{T}$, $\boldsymbol{N}$, and $\boldsymbol{B}$, respectively, through the Frenet–Serret equations (Stoker 1969)

$$\left.\begin{aligned} \boldsymbol{R}_x &= A\boldsymbol{T}, \quad A = |\boldsymbol{R}_x|, \\ \boldsymbol{T}_x &= \kappa A\boldsymbol{N}, \\ \boldsymbol{N}_x &= A(-\kappa\boldsymbol{T}+\tau\boldsymbol{B}), \\ \boldsymbol{B}_x &= -\tau A\boldsymbol{N}, \end{aligned}\right\} \tag{2.1}$$

where κ and τ are the local curvature and torsion, respectively, of the curve. Without loss of generality, we can take A to be independent of x, so that the total length of the curve is A times the variation of the independent variable x, and the arclength coordinate for the curve is $s = Ax$.

If the curve moves in space, its motion can be described by the equation

$$\boldsymbol{R}_t = \gamma\boldsymbol{T}+\alpha\boldsymbol{N}+\beta\boldsymbol{B}. \tag{2.2}$$

The functions α and β are determined by the physics of the problem, but γ is completely arbitrary since tangential velocity corresponds only to a motion of the underlying coordinate description of the curve, not to a change of shape of the curve. The parameter γ is usually chosen so that a particular coordinate system, such as arclength coordinates, is preserved along the curve. Furthermore, γ can always be chosen so that A remains independent of x for all time. Adding an arbitrary constant to γ in no way changes the shape of the solution curve

A simple example is the case $\alpha = 0$, $\beta = \kappa$, describing the self-induced motion of a vortex filament in an ideal incompressible fluid. We suppose that there is a thin

vortex tube in an incompressible fluid to which non-zero vorticity is confined. We take the tangent to the filament to be the unit vector with the same direction as the vector of the vorticity in the tube. In the limit of an infinitely thin tube, it can be shown (Batchelor 1967; Lamb 1981) that the velocity of the tube is proportional to κB, where κ is the curvature of the tube and B is its binormal vector. There is some difficulty with the derivation of this equation, since in the limit of a long infinitely thin tube, logarithmic singularities arise from the nature of the approximation, and to get rid of these unbounded logarithmic terms, a logarithmic change of timescale is made. Improvements to the model, taking into account small but finite viscosity and core size, have been made (Callegari & Ting 1978). However, for this paper, we take as our model of vortex motion the equation (2.2) with $\alpha = 0$, $\beta = \kappa$.

Another example is the equation governing the motion of a vortex filament in a superfluid. This equation is given in Schwarz (1985, 1988) as

$$\boldsymbol{R}_t = c\kappa\boldsymbol{B} + \boldsymbol{V}_s + a\boldsymbol{T}\times(\boldsymbol{V}_n - c\kappa\boldsymbol{B}) - b\boldsymbol{T}\times(\boldsymbol{T}\times(\boldsymbol{V}_n - c\kappa\boldsymbol{B})), \tag{2.3}$$

where $\boldsymbol{V}_s$ and $\boldsymbol{V}_n$ are the velocities of the superfluid and the normal fluid, respectively. The parameters a and b are temperature-dependent parameters which measure the frictional force exerted by the normal fluid on the vortex line. a and b are small numbers that have been measured experimentally, and numerical values are reported in Schwarz (1985). For example, at temperature of 1 K, $a = 0.006$ and $b = 0.003$ while at temperature of 1.5 K, $a = 0.073$, and $b = 0.018$.

If we rewrite the vector $\boldsymbol{V}_n$ as $\boldsymbol{V}_n = (\boldsymbol{V}_n\cdot\boldsymbol{T})\,\boldsymbol{T} + (\boldsymbol{V}_n\cdot\boldsymbol{N})\,\boldsymbol{N} + (\boldsymbol{V}_n\cdot\boldsymbol{B})\,\boldsymbol{B}$, it follows that the equation of motion (2.3) is equivalent to

$$\boldsymbol{R}_t = \boldsymbol{V}_s + b\boldsymbol{V}_n + (1-b)c\kappa\boldsymbol{B} + a\boldsymbol{T}\times(\boldsymbol{V}_n - c\kappa\boldsymbol{B}). \tag{2.4}$$

In a coordinate system moving with velocity $\boldsymbol{V}_s + b\boldsymbol{V}_n$, this equation takes the form of (2.2) with

$$\alpha = a(\kappa - \boldsymbol{V}_n\cdot\boldsymbol{B}), \quad \beta = c(1-b)\kappa + a(\boldsymbol{V}_n\cdot\boldsymbol{N}). \tag{2.5}$$

Notice that in the case $a = 0$, these expressions reduce to $\alpha = 0$, β proportional to κ.

It is our goal to study the behaviour of closed curves which evolve according to (2.2). One easy example is a circle. That is, if there is a value of curvature $\kappa = \kappa_0$ for which $\alpha = 0$ when $\tau = 0$, then the circle of radius $r_0 = 1/\kappa_0$ moves without change of shape in the direction normal to the plane of the circle with velocity β, evaluated at $\kappa = \kappa_0$, $\tau = 0$.

To find other solutions is is helpful to express (2.2) in a more convenient form. We wish to find the shape of solution curves without reference to a specific coordinate system, and so we seek equations of motion for the curvature and torsion that do not make reference to the position vector $\boldsymbol{R}$. To this end, we suppose the space curve $\boldsymbol{R}$ has velocity specified by (2.2). To find equations of motion for curvature and torsion we differentiate $\boldsymbol{R}_t$ in (2.2) with respect to x, and $\boldsymbol{R}_x$ in (2.1) with respect to t, and set $\boldsymbol{R}_{xt} = \boldsymbol{R}_{tx}$. We find that

$$(A\boldsymbol{T})_t = (\gamma_x - \alpha\kappa A)\,\boldsymbol{T} + (\alpha_x + \gamma\kappa A - \tau\beta A)\,\boldsymbol{N} + (\beta_x + \alpha\tau A)\,\boldsymbol{B}, \tag{2.6}$$

Since $\boldsymbol{T}$ is a unit vector for all time, $\boldsymbol{T}\cdot\boldsymbol{T}_t = 0$, from which it follows that

$$A_t = \gamma_x - \alpha\kappa A, \tag{2.7}$$

and

$$\boldsymbol{T}_t = v\boldsymbol{N} + u\boldsymbol{B}, \tag{2.8}$$

where

$$v = \frac{\alpha_x}{A} + \gamma\kappa - \tau\beta, \quad u = \frac{\beta_x}{A} + \alpha\tau. \tag{2.9}$$

Equation (2.7) determines how the coordinate system must change, and if $A = 1$, this determines how to maintain arclength coordinates. If we are looking for solutions that are invariant, it is appropriate to preserve the arclength as the independent length variable, but to study the general motion of a closed vortex filament, total length may not be preserved, and so requiring $A = 1$ would be incorrect.

Next, we differentiate $\boldsymbol{T}_t$ with respect to x and $\boldsymbol{T}_x$ with respect to t, and set $\boldsymbol{T}_{xt} = \boldsymbol{T}_{tx}$, to find that

$$(\kappa A\boldsymbol{N})_t = -\kappa vA\boldsymbol{T} + (v_x - \tau uA)\boldsymbol{N} + (u_x + \tau vA)\boldsymbol{B}. \tag{2.10}$$

Since $\boldsymbol{N}$ is a unit vector, $\boldsymbol{N}$ and $\boldsymbol{N}_t$ are orthogonal, so that

$$(\kappa A)_t = v_x - \tau uA, \tag{2.11}$$

and

$$\boldsymbol{N}_t = -v\boldsymbol{T} + z\boldsymbol{B}, \tag{2.12}$$

where

$$\kappa z = \tau v + \frac{u_x}{A}. \tag{2.13}$$

Since $\boldsymbol{T}\cdot\boldsymbol{B} = 0$, and $\boldsymbol{N}\cdot\boldsymbol{B} = 0$, it follows that $\boldsymbol{B}_t\cdot\boldsymbol{N} = -\boldsymbol{N}_t\cdot\boldsymbol{B}$, and $\boldsymbol{B}_t\cdot\boldsymbol{T} = -\boldsymbol{T}_t\cdot\boldsymbol{B}$, so that

$$\boldsymbol{B}_t = -u\boldsymbol{T} - z\boldsymbol{N}, \tag{2.14}$$

and

$$(\tau A)_t = z_x + \kappa uA. \tag{2.15}$$

In summary, if α and β are the normal and binormal velocities, respectively, of a moving curve, then the curvature, torsion and tangential velocity γ evolve according to

$$\left.\begin{aligned} &(\kappa A)_t = v_x - \tau uA, \quad (\tau A)_t = z_x + \kappa uA, \quad A_t = \gamma_x - \alpha\kappa A, \\ &v = \frac{\alpha_x}{A} + \gamma\kappa - \tau\beta, \quad u = \frac{\beta_x}{A} + \alpha\tau, \quad \kappa z = \tau v + \frac{u_x}{A}, \end{aligned}\right\} \tag{2.16}$$

As an example, in the special case $\alpha = 0, \beta = \kappa$ (which is the problem we shall study beginning in §4), (2.16) reduces substantially to

$$(\kappa^2)_t = (\gamma\kappa^2 - 2\tau\kappa^2)_s, \quad \tau_t = \left(\frac{\kappa^2}{2} + z\right)_s, \quad z\kappa = \kappa_{ss} + \tau\kappa(\gamma - \tau), \tag{2.17}$$

where γ is an arbitrary constant, and (because we can take $A = 1$) s is the arclength coordinate.

The requirement that the solution curve be closed adds to further complication. In order to know that a space curve is closed we must have that $\boldsymbol{R}$, the position vector, is a periodic function of its arclength coordinate. This implies that the curvature and torsion must be periodic, and that

$$\int_0^P \boldsymbol{T}\,dx = 0, \tag{2.18}$$

where P is the period of the periodic solution, and $\boldsymbol{T}$ is the tangent vector to the curve $\boldsymbol{R}$.

To know that (2.18) is satisfied, one must solve the evolution equations (2.16) along with the Frenet–Serret equations. Unfortunately, as stated in (2.1), the Frenet–Serret equations are not in a particularly convenient form to solve. As presented in (2.1), they are a system of twelve equations in twelve unknowns (three components for each of four vectors). Since the vectors $\boldsymbol{T}$, $\boldsymbol{N}$, and $\boldsymbol{B}$ are unit vectors,

it is more convenient to present $\boldsymbol{T}$ and $\boldsymbol{N}$ in spherical coordinates in terms of the four angles θ, η, ϕ, ψ (only three of which are independent) as

$$\boldsymbol{T}=\begin{bmatrix}\cos\phi\cos\theta\\ \cos\phi\sin\theta\\ \sin\phi\end{bmatrix}, \quad \boldsymbol{N}=\begin{bmatrix}\cos\psi\cos\eta\\ \cos\psi\sin\eta\\ \sin\psi\end{bmatrix}. \tag{2.19}$$

Here θ, η are angles in the (x,y)-plane, and ϕ, ψ denote inclination out of the (x,y)-plane. That is, the angles θ and η correspond to longitude, and angles ϕ and ψ to latitude in a spherical coordinate system. The binormal vector can be expressed in terms of these angles since $\boldsymbol{B}=\boldsymbol{T}\times\boldsymbol{N}$. It is convenient to let $\eta-\theta=\frac{1}{2}\pi+q$, and then, since $\boldsymbol{T}$ and $\boldsymbol{N}$ are orthogonal, it must be that

$$\sin\phi\sin\psi-\cos\phi\cos\psi\sin q=0. \tag{2.20}$$

This relationship determines η in terms of the three independent angular variables θ, ϕ, and ψ. Now the Frenet-Serret equations can be expressed as three equations in terms of the three angular variables θ, ϕ, and ψ as

$$\left.\begin{aligned}(\sin\phi)_x&=\kappa A\sin\psi,\\ (\sin\psi)_x&=A(\tau\cos\phi\cos\psi\cos q-\kappa\sin\phi),\\ \theta_x&=\kappa A\cos\psi\cos q/\cos\phi.\end{aligned}\right\} \tag{2.21}$$

With the change of variables $\Phi=\sin\phi$, and $\Psi=\sin\psi$, these equations simplify further to

$$\Phi_x=A\kappa\Psi, \quad \Psi_x=A(\tau X-\kappa\Phi), \quad \theta_x=\frac{A\kappa X}{1-\Phi^2}, \tag{2.22}$$

where

$$X^2+\Phi^2+\Psi^2=1.$$

In terms of these variables the vector $\boldsymbol{T}$ has components

$$\boldsymbol{T}=\begin{bmatrix}(1-\Phi^2)^{\frac{1}{2}}\cos\theta\\ (1-\Phi^2)^{\frac{1}{2}}\sin\theta\\ \Phi\end{bmatrix}. \tag{2.23}$$

This completes the formulation of the problem to be solved. To summarize, to find closed-curve solutions, we seek spatially periodic solutions of the equations of curvature and torsion (2.16). We must also solve the Frenet–Serret equations (2.22) in order to determine the tangent vector $\boldsymbol{T}$ through (2.23), and finally we require that the tangent vector have zero integral as in (2.18) so that the solution curve is closed. Throughout the remainder of this paper we shall take $\alpha=0$, and $\beta=\kappa$, as for the self-induced motion of a vortex filament, in which case the equations of motion for curvature and torsion reduce to (2.17). There are many other interesting problems with more complicated choices of α and β which will not be discussed here (see for example Keener 1988*a*, 1989; Keener & Tyson 1988).

3. Torus knots

Our goal in this section is to find solutions of the Frenet–Serret equations that are closed knotted curves. That is, we want to determine characteristics of the curvature and torsion of a curve that guarantee that the curve is closed and knotted. To do so we need to understand a few features about knotted curves.

One of the easiest ways to construct a knot is to wrap a string around a doughnut,

or torus. A torus can be described as the cross-product of two circles of radius r_1 and r_2, with $r_1 > r_2$ and corresponding angular variables ϕ and θ (not to be confused with the angles used in the last section to define the tangent and normal vectors). Any curve drawn on the surface of a torus has a winding number defined as follows:

Definition 3.1. The *winding number* for a curve on the surface of a torus, denoted as $\phi = \phi(x)$, $\theta = \theta(x)$, is the number $W = \lim_{x\to\infty} \theta(x)/\phi(x)$.

In words, the winding number is the average number of wraps of the curve around the small radius of the torus per wrap around the large radius. The winding number exists and is unique if the curve is not self-intersecting, and is an invariant for the curve. That is, if the curve is deformed without self-intersections into another curve, the winding number is unchanged.

The important fact about knots that we will use is Massey (1967).

THEOREM 3.2. *A closed non-self-intersecting curve on the surface of a torus with winding number m/n, m and n relatively prime, $m > n > 1$, is a non-trivial knot.*

A trefoil knot is one with winding number 3/2, that is, three wraps around the small radius of the torus for two wraps around the large radius of the torus. In figure 1(*a*) is shown a left-handed trefoil knot (solid line) with the centreline of a circular torus (dashed line) though it. In figures 1(*b*) and 1(*c*) are shown 5/2 (also called the Solomon's seal) and 4/3 torus knots, respectively. Any knot constructed as a wrapping of a torus is called a torus knot, but in the class of all knots, torus knots comprise only a very small subclass. In §6 we shall discuss one class of more complicated knots, the cabled, or iterated, torus knots.

Not that we know how to describe a simple torus knot, the bifurcation picture can be explored. How might we construct a torus knot as a solution of a differential equation as a bifurcation from a simpler solution curve? The answer is found by examining the opposite question of how a knot might be turned into some simpler structure. Notice that if the small radius of a torus is allowed to approach zero the torus approaches a circle and the knot becomes an n cover of the circle with the curve twisted around itself m times. To undo this collapse we should look for a curve whose curvature and torsion oscillate with very small amplitude m times as a circle is traversed n times, with m and n relatively prime.

To see how this works we solve a practice problem. Suppose the curvature and torsion of some nearly circular closed curves are known, and suppose that the curvature and torsion are small-amplitude oscillatory functions that oscillate m times as the circle is traversed n times. We shall show how to find a closed-curve solution of the Frenet–Serret equations and that the resulting curve is a torus knot with winding number m/n. To be specific, we suppose that the curvature and torsion of the curve are given by (to leading order in some small parameter ϵ)

$$\left.\begin{aligned} \kappa(x) &= \kappa_0 + \epsilon a \sin \mu x + \epsilon b \cos \mu x, \\ \tau(x) &= \tau_0 + \epsilon c \cos \mu x, \end{aligned}\right\} \tag{3.1}$$

where $\mu = \kappa_0 m/n$. Here we take the independent variable x to vary over the fixed interval $0 \leqslant x \leqslant 2\pi n/\kappa_0$. We seek solutions of the Frenet–Serret equations (2.22) that are closed curves for ϵ small, and use $A = A(\epsilon)$ to adjust the total length of the curve and $\tau_0 = \tau_0(\epsilon)$ to adjust the average value of torsion so that the curve is closed.

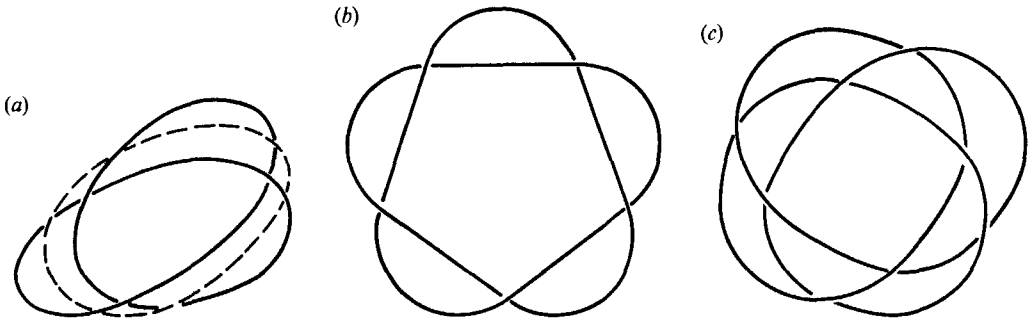

FIGURE 1. Three examples of torus knots: (*a*) a trefoil knot (solid curve) with the central filament of its interior torus (dashed); (*b*) a 5:2 torus knot (Solomon's seal); and (*c*) a 4:3 torus knot.

It is an easy matter to show that closed-curve solutions for this problem exist. In fact, using the implicit function (Keener 1988*b*), one can readily show:

THEOREM 3.3. *Suppose that* $\kappa_1(x)$ *and* $\tau_1(x)$ *are periodic functions of period* P, *and that there are integers* m *and* n *so that* $mP\kappa_0 = 2n\pi$. *Suppose further that*

$$\left.\begin{aligned} &\int_0^{mP} \kappa_1(x)\sin\kappa_0 x\,\mathrm{d}x = 0, \quad \int_0^{mP} \kappa_1(x)\cos\kappa_0 x\,\mathrm{d}x = 0, \\ &\int_0^{mP} \tau_1(x)\sin\kappa_0 x\,\mathrm{d}x = 0, \quad \int_0^{mP} \tau_1(x)\cos\kappa_0 x\,\mathrm{d}x = 0, \quad \int_0^{mP} \tau_1(x)\,\mathrm{d}x = 0. \end{aligned}\right\} \tag{3.2}$$

Then for all ϵ *sufficiently small, there are functions* $A = A(\epsilon)$ *and* $\tau_0 = \epsilon^2\tau_2(\epsilon)$, *and a closed curve whose curvature and torsion are given by*

$$\kappa(x) = \kappa_0 + \epsilon\kappa_1(x), \quad \tau(x) = \epsilon\tau_1(x) + \epsilon^2\tau_2(\epsilon). \tag{3.3}$$

The arclength variable for the curve is $s = A(\epsilon)\,x$.

The solution of our practice problem and the proof of this theorem follow from a straightforward regular perturbation and application of the implicit function theorem. We assume that the variables for (2.22) have power series expansions in ϵ of the form

$$\left.\begin{aligned} \Phi(x) &= \epsilon\Phi_1(x) + \epsilon^2\Phi_2(x) + \dots, \\ \Psi(x) &= \epsilon\Psi_1(x) + \epsilon^2\Psi_2(x) + \dots, \\ \theta(x) &= \kappa_0 x + \epsilon\theta_1(x) + \epsilon^2\theta_2(x) + \dots, \end{aligned}\right\} \tag{3.4}$$

where $A = 1 + \epsilon A_1 + \epsilon^2 A_2 + \dots$. For $\epsilon = 0$, this corresponds to a closed circle with curvature κ_0. For small ϵ, the tangent vector is given approximately by

$$\boldsymbol{T} = \begin{bmatrix} \cos\kappa_0 x \\ \sin\kappa_0 x \\ 0 \end{bmatrix} + \epsilon \begin{bmatrix} -\theta_1(x)\sin\kappa_0 x \\ \theta_1(x)\cos\kappa_0 x \\ \Phi_1(x) \end{bmatrix} + \dots. \tag{3.5}$$

We expand the Frenet–Serret equations (2.22) into powers of ϵ and collect like powers of ϵ. The leading-order equations are given by

$$\frac{\mathrm{d}\Phi_1}{\mathrm{d}x} = \kappa_0\Psi_1, \quad \frac{\mathrm{d}\Psi_1}{\mathrm{d}x} = -\kappa_0\Phi_1 + \tau_1(x), \quad \frac{\mathrm{d}\theta_1}{\mathrm{d}x} = A_1\kappa_0 + \kappa_1(x). \tag{3.6}$$

We seek periodic solutions of (3.6) with period $mP = 2n\pi/\kappa_0$. These exist if and only if solvability conditions are satisfied, namely, if and only if $\tau_1(x)$ is orthogonal to both $\sin\kappa_0 x$ and $\cos\kappa_0 x$ on the interval $0 \leqslant x \leqslant mP$, and

$$A_1\kappa_0 = -\int_0^{mP} \kappa_1(x)\,dx. \tag{3.7}$$

If the average value of $\kappa_1(x)$ is zero, we pick $A_1 = 0$. Furthermore, we require that the integral of the tangent vector $\boldsymbol{T}$ be zero. To first order in ϵ, this implies that $\kappa_1(x)$ must be orthogonal to $\sin\kappa_0 x$ and $\cos\kappa_0 x$, and that the average value of $\tau_1(x)$ must be zero on the interval $0 \leqslant x \leqslant mP$.

To carry out the perturbation scheme, we must have enough adjustable free parameters to satisfy periodicity requirements at each order of the perturbation scheme. Two free parameters are necessary. The scale factor $A = A(\epsilon)$ is used to ensure that $\theta(x)$ is periodic, and the avarage value of τ is used to ensure that the average value of Φ is also zero. These observations are sufficient to allow us to write (2.22), (2.23) and (2.18) (via a standard use of the Lyapunov–Schmidt technique) in a form to which the implicit function theorem can be directly applied, guaranteeing that there is a solution of the full problem for all ϵ sufficiently small (Chow & Hale 1982; Keener 1988*b*).

For the special example (3.1) where the curvature and torsion are simple trigonometric functions, we can solve the leading-order equations explicitly. We find that the leading order solution is given by

$$\left.\begin{aligned} \Phi_1(x) &= \frac{c\kappa_0}{\kappa_0^2-\mu^2}\cos\mu x, \\ \Psi_1(x) &= \frac{c\kappa_0}{\mu(\mu^2-\kappa_0^2)}\sin\mu x, \\ \theta_1(x) &= -\frac{a}{\mu}\cos\mu x + \frac{b}{\mu}\sin\mu x. \end{aligned}\right\} \tag{3.8}$$

Integrating the tangent vector, we find a position vector $\boldsymbol{R}$ with components r_1, r_2, r_3 given by

$$\left.\begin{aligned} r_1(x) &= \frac{1}{\kappa_0}\sin\kappa_0 x + \frac{\epsilon}{\kappa_0^2-\mu^2}\left(b\left(\frac{\kappa_0}{\mu}\cos\kappa_0 x\sin\mu x - \sin\kappa_0 x\cos\mu x\right)\right. \\ &\quad \left. -a\left(\frac{\kappa_0}{\mu}\cos\kappa_0 x\cos\mu x + \sin\kappa_0 x\sin\mu x\right)\right), \\ r_2(x) &= -\frac{1}{\kappa_0}\cos\kappa_0 x + \frac{\epsilon}{\kappa_0^2-\mu^2}\left(b\left(\cos\kappa_0 x\cos\mu x + \frac{\kappa_0}{\mu}\sin\kappa_0 x\sin\mu x\right)\right. \\ &\quad \left. +a\left(\cos\kappa_0 x\sin\mu x - \frac{\kappa_0}{\mu}\sin\kappa_0 x\cos\mu x\right)\right), \\ r_3(x) &= \frac{\epsilon\kappa_0 c}{\mu(\kappa_0^2-\mu^2)}\sin\mu x, \end{aligned}\right\} \tag{3.9}$$

to leading order in ϵ. At each order in the perturbation calculation, the coefficient A_i is used to guarantee that $\theta(x) - \kappa_0 x$ is a periodic function, and the average value of

torsion must be adjusted so that the curve is closed. With a bit more work, one can show that

$$\left.\begin{aligned} A(\epsilon) &= 1-\frac{\epsilon^2 c^2}{4(\kappa_0^2-\mu^2)}+\ldots, \\ \frac{1}{mP}\int_0^{mP}\tau(x)\,\mathrm{d}x &= -\frac{bc\kappa_0\epsilon^2}{2(\mu^2-\kappa_0^2)}+\ldots. \end{aligned}\right\} \tag{3.10}$$

The first of these shows how the length of the curve changes as a function of ϵ. In fact, since $\mu > \kappa_0$, $A(\epsilon)$ is greater than one, so that for non-zero ϵ the arclength of the curve is $2n\pi A(\epsilon)/\kappa_0$, which is slightly greater than $2n\pi/\kappa_0$.

Now we can verify that for ϵ small, the curve $\boldsymbol{R}$ is indeed a torus knot. This is done by showing that the curve $\boldsymbol{R}$ lies on a torus and by calculating its winding number. To see that this is a curve on a torus, we rewrite the curve $\boldsymbol{R}(x)$ in toroidal coordinates as $\boldsymbol{R}(x) = \boldsymbol{R}_0(t)+\alpha(t)\,\boldsymbol{N}(t)+\beta(t)\,\boldsymbol{B}(t)$, where $\boldsymbol{R}_0(t)$ is the centreline of the torus, $\boldsymbol{N}$ and $\boldsymbol{B}$ are the normal and binormal vectors for the centreline $\boldsymbol{R}_0(t)$, and t is some function of x. We take the centreline $R_0(t)$ to have components

$$r_{01}(t) = \frac{1}{\kappa_0}\sin\kappa_0 t, \quad r_{02}(t) = -\frac{1}{\kappa}\cos\kappa_0 t, \quad r_{03}(t) = 0, \tag{3.11}$$

which is a circle. We choose t as a function of x by requiring that the tangent vector of $\boldsymbol{R}_0(t)$ be orthogonal to the vector $\boldsymbol{R}(x)$, that is, $r_1(x)\cos\kappa_0 t + r_2(x)\sin\kappa_0 t = 0$. It follows that

$$\begin{aligned} \sin\kappa_0(x-t)+\frac{\epsilon\kappa_0}{\mu(\kappa_0^2-\mu^2)}&(b(\kappa_0\sin\mu x\cos\kappa_0(x-t)-\mu\cos\mu x\sin\kappa_0(x-t)) \\ &-a(\kappa_0\cos\mu x\cos\kappa_0(x-t)+\mu\sin\mu x\sin\kappa_0(x-t)))=0, \end{aligned} \tag{3.12}$$

or to leading order in ϵ, $x = t$. Now, to calculate the coordinate amplitude $\alpha(t)$, we note that $1-\kappa_0\alpha(t) = \kappa_0^2\,\boldsymbol{R}(x)\cdot\boldsymbol{R}_0(t)$, so that

$$\begin{aligned} \alpha(t) = \frac{\epsilon}{\mu(\mu^2-\kappa_0^2)}&[a(\kappa_0\cos\mu x\sin\kappa_0(x-t)-\mu\sin\mu x\cos\kappa_0(x-t)) \\ &-b(\kappa_0\sin\mu x\sin\kappa_0(x-t)+\mu\cos\mu x\cos\kappa_0(x-t))], \end{aligned} \tag{3.13}$$

or to leading order in ϵ,

$$\alpha(t) = -\frac{\epsilon}{\mu^2-\kappa_0^2}(a\sin\mu x + b\cos\mu x). \tag{3.14}$$

Of course, $\beta(t)$ is the z-component of $\boldsymbol{R}$ so that

$$\beta(t) = -\frac{\epsilon\kappa_0 c}{\mu(\mu^2-\kappa_0^2)}\sin\mu x. \tag{3.15}$$

The trajectory of the curves $\alpha(t)$, $\beta(t)$ determines the behaviour of the curve in the plane orthogonal to the centreline. This trajectory satisfies the equation

$$(c\kappa_0\alpha - a\mu\beta)^2 + (b\mu\beta)^2 = \left(\frac{cb\kappa_0\epsilon}{\mu^2-\kappa_0^2}\right)^2. \tag{3.16}$$

It follows that if b and c are non-zero, the curve $\boldsymbol{R}$ lies on a torus with elliptical cross-section. Furthermore, it is apparent that the ellipse is traversed in a single direction m times for every n times that the circular centreline $\boldsymbol{R}_0(t)$ is traversed, so that the winding number is m/n, as promised. If b or c is zero, higher-order terms are needed to determine if there is rotation about a torus. We can determine from (3.14) and

(3.15) that the ellipse is traversed in a clockwise direction as x increases if b and c have the same signs, corresponding to a right-handed knot. If b and c have opposite signs, the ellipse is traversed in the counterclockwise direction so that the knot is left handed. We summarize the result of this calculation in

THEOREM 3.4. *Suppose that the functions $\kappa_1(x,\epsilon)$ and $\tau_1(x,\epsilon)$ are periodic in x with period $P = 2\pi n/m\kappa_0$, with m/n an irreducible rational number greater than one. Suppose further that*

$$\kappa_1(x,\epsilon) = a\sin\mu x + b\cos\mu x + O(\epsilon), \quad \tau_1(x,\epsilon) = c\cos\mu x + O(\epsilon),$$

with

$$\int_0^P \kappa_1(x,\epsilon)\,dx = \epsilon\kappa_2(\epsilon), \quad \int_0^P \tau_1(x,\epsilon)\,dx = 0.$$

For all ϵ sufficiently small there are functions $A(\epsilon)$ and $\tau_2(\epsilon)$ so that the curve with curvature and torsion given by

$$\kappa(x) = \kappa_0 + \epsilon\kappa_1(x,\epsilon), \quad \tau(x) = \epsilon\tau_1(x,\epsilon) + \epsilon^2\tau_2(\epsilon)$$

is a closed curve with arclength variable $s = A(\epsilon)x$. Furthermore,

$$A(\epsilon) = 1 + \epsilon^2\left(\frac{c^2}{4(\mu^2-\kappa_0^2)} - \frac{\kappa_2(0)}{\kappa_0}\right) + \dots,$$

$$\tau_2(\epsilon) = -\frac{bc\kappa_0}{2(\mu^2-\kappa_0^2)} + \dots.$$

If $bc \neq 0$, the curve $\boldsymbol{R}$ is a closed torus knot with winding number m/n for all non-zero ϵ sufficiently small. Furthermore, the knot is right handed if $bc > 0$, and left handed if $bc < 0$.

4. Invariant knotted vortex filaments

Now comes the task of determining when (or if) the equations governing the structure of a vortex filament have oscillatory curvature and torsion of the correct type. This we can do using a standard perturbation analysis. The equations to be solved are

$$(\kappa^2)_t = (\gamma\kappa^2 - 2\tau\kappa^2)_s, \quad \tau_t = (\tfrac{1}{2}\kappa^2 + z)_s, \quad z\kappa = \kappa_{ss} + \tau\kappa(\gamma - \tau), \tag{4.1}$$

where γ is an arbitrary constant, and s is the arclength coordinate.

Because of Theorem 3.4 we know something about the form of the solutions we are seeking. First, since we do not yet know the length of the curve it is advantageous to make a change of lengthscale in (4.1), allowing us to work on a fixed spatial interval keeping the total length of the curve as a free parameter.

Second, notice that for a periodic solution we can adjust the average value of the torsion as we wish. This is because, according to (4.1), the average torsion is a constant independent of time, and furthermore, (4.1) are invariant under the transformation

$$\tau \Rightarrow \tau + \tau_0, \quad \gamma \Rightarrow \gamma + \gamma_0, \quad z \Rightarrow z + (\gamma_0 - 2\tau_0)\tau + (\gamma + \gamma_0 - \tau_0)\tau_0, \quad x \Rightarrow x + (2\tau_0 - \gamma_0)t. \tag{4.2}$$

for arbitrary constants τ_0 and γ_0. Thus, we can adjust the average value of torsion simply by making a change of spatial coordinate system into the appropriate travelling frame of reference.

Finally, any small-amplitude solution of (4.1) can be made to correspond to a closed-curve solution. This follows since (4.1) are invariant under the transformation

$$\kappa \Rightarrow a\kappa, \quad \tau \Rightarrow a\tau, \quad \gamma \Rightarrow a\gamma, \quad z \Rightarrow a^2 z, \quad x \Rightarrow x/a, \quad t \Rightarrow t/a^2. \tag{4.3}$$

Thus, any period-P solution whose curvature has average value κ_0 can be transformed by a change of scale into a period $P' = aP$ solution with average curvature $\kappa_0' = a\kappa_0$, and then the restriction on period from Theorem 3.4 that $P'\kappa_0' = 2\pi n/m$ is readily satisfied with an appropriate choice of a.

We begin our analysis of (4.1) by looking for invariant solutions, that is, solutions of (4.1) that are independent of time. These are travelling wave solutions of (4.1), where the speed of translation is given by the unknown constant γ. It is convenient to work on a fixed spatial interval, so we introduce the change of spatial scale $s = Ax$. The parameter A will be determined by the condition that the curve be closed, as given in Theorem 3.4. The resulting equations are

$$\gamma\kappa^2 - 2\tau\kappa^2 = C_1, \quad \kappa^2 + 2z = C_2, \quad \kappa_{xx} = A^2(z\kappa - \tau\kappa(\gamma - \tau)), \tag{4.4}$$

where the constants C_1 and C_2 are undetermined constants of integration. One can write (4.4) as a single equation for the quantity $u = \kappa^2$, of the form

$$u'' = A^2(C_3 + (C_2 - \tfrac{1}{2}\gamma^2)u - \tfrac{3}{4}u^2), \tag{4.5}$$

where C_3 is another unknown constant. Exact solutions of this equation can be written out in terms of elliptic functions (Kida 1981). For our purposes, however, it is more useful to express solutions as perturbations of a constant solution. To do this, we observe that $\kappa = \kappa_0$, $\tau = 0$, $z = 0$, is a solution of (4.4) for any constant $\gamma = \gamma_0$. To see what kinds of spatially periodic solutions are possible in a neighbourhood of this constant solution, we linearize (4.4) about the known constant solution and find

$$\kappa_{1xx} + (\kappa_0^2 + \gamma_0^2)\kappa_1 = c_1\gamma_0 + c_2\kappa_0, \quad \gamma_0\kappa_1 - \kappa_0\tau_1 = c_1, \quad z_1 + \kappa_0\kappa_1 = c_2, \tag{4.6}$$

where κ_1, τ_1, and z_1 are the small deviations of κ, τ and z from the constant solution. We pick the constants $c_1 = 0$, and $c_2 = 0$, so that the average curvature and average torsion are zero, and then find that

$$\kappa_{1xx} + (\kappa_0^2 + \gamma_0^2)\kappa_1 = 0, \quad \kappa_0\tau_1 = \gamma_0\kappa_1. \tag{4.7}$$

The solutions of (4.7) are of the form

$$\kappa_1(x) = a\kappa_0 \cos\mu x, \quad \tau_1(x) = a\gamma_0 \cos\mu x, \tag{4.8}$$

provided $\gamma_0^2 = \mu^2 - \kappa_0^2$. Here we see exactly the structure for which we had hoped. Namely, for any value of μ that is a rational multiple of κ_0, $\mu = m\kappa_0/n$, we can choose the speed of translation γ_0 so that $\gamma_0^2 = \mu^2 - \kappa_0^2$, and the solution of the linearized equations has curvature and torsion which, according to Theorem 3.4, give rise to an m/n torus knot.

The calculation of the knotted solution is a standard perturbation calculation (see Cole 1968; Keener 1988*b*) which we will not belabour. Since the linearized equations have a periodic solution at value γ_0, we look for periodic solutions of the governing equations with γ in a neighbourhood of γ_0. We seek a power series solution of (4.4) in powers of some small parameter ϵ of the form

$$\left.\begin{aligned} \kappa(x) &= \kappa_0 + \epsilon\kappa_0 \cos\mu x + \epsilon^2\kappa_2(x) + \dots, \\ \tau(x) &= \epsilon\gamma_0 \cos\mu x + \epsilon^2\tau_2(x) + \dots. \end{aligned}\right\} \tag{4.9}$$

We know already from the form of this solution and the statement of Theorem 4.3 that we must take the scale factor $A(\epsilon)$ and average torsion to satisfy

$$A(\epsilon) = 1 + \tfrac{1}{4}\epsilon^2 + \ldots, \quad \frac{1}{P}\int_0^P \tau_2(x)\,dx = -\frac{\epsilon^2\kappa_0^2}{2\gamma_0}. \tag{4.10}$$

We also expand the parameter γ as $\gamma_0 + \epsilon^2\gamma_2 + \epsilon^4\gamma_4 + \ldots$.

The perturbation calculation is straightforward in concept, but tedious in details. We expand (4.4) in powers of ϵ, collect coefficients of like powers of ϵ, and then solve the resulting hierarchy of equations sequentially. Unknown parameters are determined by requiring the solution to be periodic (equivalently, by invoking the Fredholm Alternative). This calculation was done using the algebraic programming language REDUCE, so we present only the results of the calculation. We find that

$$\left.\begin{aligned} \kappa_2(x) &= \frac{\kappa_0(2\kappa_0^2-\mu^2)}{4\mu^2}\cos 2\mu x, \\ \tau_2(x) &= -\frac{\kappa_0^2}{2\gamma_0} + \frac{\gamma_0(\kappa_0^2-2\mu^2)}{2\mu^2}\cos 2\mu x, \\ 4\gamma_2\gamma_0\mu^2 &= -(\mu^4+\kappa_0^2\mu^2+3\kappa_0^4). \end{aligned}\right\} \tag{4.11}$$

Taken in conjunction with the results of the previous section, we see that for γ in a one-sided neighbourhood of γ_0 (determined by the sign of γ_2), there are closed knotted invariant solutions of the equations of motion (4.1). Furthermore, if γ is positive, the knot is right handed, while if γ is negative, the knot is left handed. Note that γ determines the rate and direction of rotation of the knot about its axis of symmetry. That is, γ is the speed of translation of the knot along its tangential direction. Thus, when γ is positive, the knot rotates in the direction of its tangent vector, and with γ negative, the knot rotates in the direction opposite to its tangent vector. In other words, a right-handed knot rotates in the direction of its tangent vector, and a left-handed knot rotates in the direction opposite its tangent vector. The orientation of the tangent vector also determines the orientation of the binormal vector, and the knot moves as a rigid body in the direction of the binormal to the circle which underlies the torus knot.

5. The dynamics of torus knots

The calculation of the previous section raises a number of interesting subsidiary questions. We have shown that there are torus knots with any winding number that move as rigid bodies under the dynamics $\boldsymbol{R}_t = \kappa\boldsymbol{B}$. (Recall that the addition of a tangential component to the motion has no influence on the shape of the solution, so we do not include a tangential term here.) One would also like to know something about the stability of these invariant solutions (Kida 1982).

The invariant solutions are interesting in that they are a type of solitary structure. It is well known that the equations of motion for curvature and torsion (4.1) can be transformed into the nonlinear Schrödinger equation (Hasimoto 1972; Lamb 1981). Thus, the invariant knots correspond to spatially periodic invariant travelling wave solutions of the nonlinear Schrödinger equation. Since the nonlinear Schrödinger equation is completely integrable and has solutions which can be found using the inverse scattering transform, we know that the invariant solutions act as solitons and can be 'superposed' to find temporally quasi-periodic, spatially periodic solutions

(Tracy & Chen 1988). By analogy we wish to determine how the invariant knotted solution curves can be viewed as 'solitons' which can be superposed to give closed curves which are not invariant and may even have a different topology from the invariant torus knots.

In this section we shall explore the behaviour of the simplest 'two-soliton' solutions, and in §6 we study the behaviour of the simplest 'four-soliton' solutions. As we saw in §4, the simple solitary wave solution corresponds to an invariant torus knot that rotates around its axis of symmetry at some speed. We also learned that for each rational number m/n there are left-handed and right-handed torus knots that rotate about their axes of symmetry in opposite directions. If we start the evolution $\boldsymbol{R}_t = \kappa \boldsymbol{B}$ with an arbitrary torus knot, we do not expect the motion to be invariant, although the total length will not change and the curve will remain closed. We do not know, however, if the topology of the knot will remain the same or if there will be self-intersections and crossings of the curve which change its topology. There is certainly nothing in the equations of motion that precludes intersections of different pieces of the curve, since the equations of motion only take into account local effects.

To get some idea of the evolution of an 'arbitrary' torus knot, we seek solutions of the evolution equations (4.1). The solutions we find will be periodic in space, and small amplitude in their deviation from a circle. We seek solutions of (4.1) using the method of harmonic balance (Stoker 1966). Specifically, we suppose that solutions can be written in the form

$$\left.\begin{aligned}
\kappa(x,t,\epsilon) &= \kappa_0(t,\epsilon) + \sum_{j=1}^{\infty} \epsilon^j (\kappa_j(t,\epsilon)\, \mathrm{e}^{\mathrm{i}j\mu x} + \kappa_j^*(t,\epsilon)\, \mathrm{e}^{-\mathrm{i}j\mu x}),\\
\tau(x,t,\epsilon) &= \tau_0(\epsilon) + \sum_{j=1}^{\infty} \epsilon^j (\tau_j(t,\epsilon)\, \mathrm{e}^{\mathrm{i}j\mu x} + \tau_j^*(t,\epsilon)\, \mathrm{e}^{-\mathrm{i}j\mu x}),\\
z(x,t,\epsilon) &= z_0(t,\epsilon) + \sum_{j=1}^{\infty} \epsilon^j (z_j(t,\epsilon)\, \mathrm{e}^{\mathrm{i}j\mu x} + z_j^*(t,\epsilon)\, \mathrm{e}^{-\mathrm{i}j\mu x}),
\end{aligned}\right\} \tag{5.1}$$

where a superscript asterisk denotes the complex conjugate. We take $\gamma = 0$, and expand $A(\epsilon)$ into powers of ϵ, as required by Theorem 3.4. We substitute (5.1) into the (4.1), and collect like exponential terms, to find the equations

$$\frac{\mathrm{d}\kappa_0}{\mathrm{d}t} = \mathrm{i}\mu\epsilon^2(\tau_1\kappa_1^* - \kappa_1\tau_1^*), \quad \kappa_0 z_0 = -\epsilon^2(\kappa_1 z_1^* + \kappa_1^* z_1 + 2\kappa_0\tau_1\tau_1^*), \tag{5.2}$$

$$\left.\begin{aligned}
\frac{\mathrm{d}\kappa_1}{\mathrm{d}t} + \mathrm{i}\mu(\kappa_0\tau_1 + 2\tau_0\kappa_1) &= \mathrm{i}\mu\epsilon^2(\kappa_0\tau_1 A_2 - 3\kappa_2\tau_1^*),\\
\frac{\mathrm{d}\tau_1}{\mathrm{d}t} - \mathrm{i}\mu(\kappa_0\kappa_1 + z_1) &= \mathrm{i}\mu\epsilon^2(\kappa_2\kappa_1^* - A_2 z_1 - A_2\kappa_0\kappa_1),\\
z_1\kappa_0 + \mu^2\kappa_1 + 2\kappa_0\tau_0\tau_1 + z_0\kappa_1 + \epsilon^2(2\kappa_0\tau_2\tau_1^* - 2A_2\mu^2\kappa_1 &\\
+ 2\kappa_1\tau_1\tau_1^* + \kappa_1^*\tau_1^2 + \kappa_1^* z_1 + \kappa_1 z_1^*) &= 0,
\end{aligned}\right\} \tag{5.3}$$

$$\left.\begin{aligned}
\frac{\mathrm{d}\kappa_2}{\mathrm{d}t} + 2\mathrm{i}\mu\kappa_0\tau_2 = -3\mathrm{i}\mu\kappa_1\tau_1, \quad \frac{\mathrm{d}\tau_2}{\mathrm{d}t} - 2\mathrm{i}\mu(\kappa_0\kappa_2 + z_2) &= \mathrm{i}\mu\kappa_1^2,\\
\kappa_0 z_2 + 4\mu^2\kappa_2 + z_1\kappa_1 + \kappa_0\tau_1^2 &= 0,
\end{aligned}\right\} \tag{5.4}$$

where we have retained only terms up to order ϵ^2.

We can approximate the solutions of these equations using multiscale techniques

given in Cole (1968) and Keener (1988*b*). Setting $\epsilon = 0$ in (5.2) and (5.3), we find that the behaviour of the solution to leading order is governed by the equations

$$\frac{d\kappa_1}{dt} = -i\mu\kappa_0\tau_1, \quad \frac{d\tau_1}{dt} = i\mu(\kappa_0^2-\mu^2)\frac{\kappa_1}{\kappa_0}, \tag{5.5}$$

with $z_0 = \tau_0 = 0$, and κ_0 constant. It is no surprise that these equations have two linearly independent solution pairs, corresponding to the two invariant solutions found in §4. However, the general solution of (5.5) is a linear combination of the two solutions, given by

$$\kappa_1(t) = \kappa_- e^{-i\omega t}+\kappa_+ e^{i\omega t}, \quad \tau_1(t) = \frac{\omega}{\mu\kappa_0}(\kappa_- e^{-i\omega t}-\kappa_+ e^{i\omega t}), \tag{5.6}$$

with κ_+ and κ_- arbitrary constants (determined from initial data), and with $\omega^2 = \mu^2(\mu^2-\kappa_0^2)$. In view of the form of (5.1), this corresponds to the superposition of two travelling waves moving in opposite directions with speed $\omega/\mu = \gamma$.

To determine the effect of the order-ϵ^2 correction terms on this solution, we make the usual two-timing assumption, that the behaviour of the solution can be described in terms of two timescales, a fast time t, and a slow time $\sigma = \epsilon^2 t$. We rewrite (5.2), (5.3), (5.4) in terms of these two time-like variables by invoking the chain rule and setting

$$\frac{d}{dt} = \frac{\partial}{\partial t}+\epsilon^2\frac{\partial}{\partial\sigma}. \tag{5.7}$$

Now the solution to leading order is given by (5.6), with the modification that κ_- and κ_+ depend on σ, that is, they are slowly varying functions of time.

The next steps follow standard perturbation arguments. We expand the unknown functions as power series in ϵ, and then require that the equations of motion have solutions that are periodic in the fast variable t at each order of ϵ. For example, we expand $\kappa_0(t)$ as $\kappa_0+\epsilon^2\kappa_{02}(t,\sigma)$, and the equation governing $\kappa_{02}(t,\sigma)$ is

$$\frac{\partial\kappa_{02}}{\partial t} = i\mu(\tau_{10}\kappa_{10}^*-\kappa_{10}\tau_{10}^*). \tag{5.8}$$

In addition, we require that the solution curve be closed, and from Theorem 3.4 we realize that

$$\tau_0 = -\frac{\epsilon^2\kappa_0}{\mu^2-\kappa_0^2}(\kappa_1\tau_1^*+\kappa_1^*\tau_1), \quad A_2 = \frac{\tau_1\tau_1^*}{\mu^2-\kappa_0^2}-\frac{\kappa_{02}}{\kappa_0},$$

to leading order in ϵ. The requirement that solutions be periodic in t leads to the differential equations for the slow evolution of the functions κ_- and κ_+,

$$\left.\begin{aligned}\kappa_0^2\omega\frac{\partial\kappa_-}{\partial\sigma} &= i(p_1(\mu)|\kappa_-|^2-p_2(\mu)|\kappa_+|^2)\kappa_-,\\ \kappa_0^2\omega\frac{\partial\kappa_+}{\partial\sigma} &= i(p_2(\mu)|\kappa_-|^2-p_1(\mu)|\kappa_+|^2)\kappa_+,\end{aligned}\right\} \tag{5.9}$$

where $$p_1(\mu) = 3\kappa_0^4+2\mu^4, \quad p_2(\mu) = 2\mu^2(3\kappa_0^2-\mu^2).$$

The solution of these equations is now easy to describe. We find that

$$\kappa_0(t) = \kappa_0-\frac{\epsilon^2}{\kappa_0}(\kappa_+(\sigma)\kappa_-^*(\sigma)e^{2i\omega t}+\kappa_-(\sigma)\kappa_+^*(\sigma)e^{-2i\omega t}), \tag{5.10}$$

and $$\kappa_+(\sigma) = \kappa_+(0)\,e^{i\omega_2(|\kappa_+|,|\kappa_-|)\,\sigma}, \quad \kappa_-(\sigma) = \kappa_-(0)\,e^{-i\omega_2(|\kappa_-|,|\kappa_+|)\,\sigma},$$

where $$\omega_2(x,y) = \frac{1}{\kappa_0^2\omega}(p_2(\mu)y^2 - p_1(\mu)\,x^2).$$

Clearly the amplitudes of κ_+ and κ_- are constant. It follows that

$$\tau_0(\epsilon) = \frac{2\mu\epsilon^2}{\omega}(|\kappa_+|^2 - |\kappa_-|^2), \quad A_2 = \frac{1}{\kappa_0^2}(|\kappa_+|^2 + |\kappa_-|^2) \tag{5.11}$$

are both constant.

We need to understand what this tells us about the evolution of torus knots. We first observe that the evolution of the curvature and torsion of the knot look very much like the superposition of two travelling waves. To this order in ϵ, the amplitudes of curvature and torsion are not affected by the interaction, but the speed of progression of the waves is affected, through the function ω_2, by the interaction. From the form of (5.1), (5.6), and (5.10), we calculate that the speed of propagation of the κ_+ wave component is

$$c_+ = -\left(\gamma_0 + \frac{\epsilon^2}{\kappa_0^2\mu^2\gamma_0}(\mu^2(5\kappa_0^2 - \mu^2)\,|\kappa_-|^2 - (3\kappa_0^2 + \kappa_0^2\mu^2 + \mu^4)\,|\kappa_+|^2)\right), \tag{5.12}$$

with a similar expression for the speed of the κ_- wave component. These speeds agree with the speed of the invariant solution (found in §4) in the case that only one of the components is non-zero.

To understand something about the shape and topology of the knots we make two observations. First, from (5.10) we know that the solution curve lies on a torus whose large radius is oscillatory, so that the whole torus is 'breathing'.

Second, by comparing (5.1) and (5.6) with (3.1) we can determine the topology of the solution curve. To do so we must determine the appropriate scalars a, b, and c so that the solution (5.1), (5.6) can be written, with a shift of independent variable x, in the form of (3.1). In other words, we must find constants c and a phase shift θ, so that $2\tau_1 = c\,e^{i\theta}$, and then find a and b so that $2\kappa_1 = (b - ia)\,e^{i\theta}$. The solution of this problem is straightforward. We write

$$\kappa_1 = |\kappa_+|\,e^{i\phi_+} + |\kappa_-|\,e^{i\phi_-}, \quad \tau_1 = \frac{\omega}{\mu\kappa_0}(|\kappa_-|\,e^{i\phi_-} - |\kappa_+|\,e^{i\phi_+}), \tag{5.13}$$

and calculate that

$$\left.\begin{aligned} c^2 &= 4\left(\frac{\omega}{\mu\kappa_0}\right)(|\kappa_+|^2 + |\kappa_-|^2 - 2|\kappa_+|\,|\kappa_-|\cos(\phi_+ - \phi_-)),\\ ac &= 8\frac{\omega}{\mu\kappa_0}|\kappa_+|\,|\kappa_-|\sin(\phi_+ - \phi_-),\\ bc &= 4\left(\frac{\omega}{\mu\kappa_0}\right)(|\kappa_+|^2 - |\kappa_-|^2). \end{aligned}\right\} \tag{5.14}$$

Recalling that $|k_+|$ and $|\kappa_-|$ are constant in time, we see that the quantity bc is a constant independent of time. From Theorem 3.4 we conclude that if $bc \neq 0$, the topology of the knot is invariant. Therefore, if $|\kappa_+|$ is larger than $|\kappa_-|$ we have a right-handed torus knot, while if $|\kappa_+|$ is smaller than $|\kappa_-|$ we have a left-handed knot, and this topology does not change during the course of the motion of the curve.

It is a bit difficult to visualize the actual motion of the torus know without some

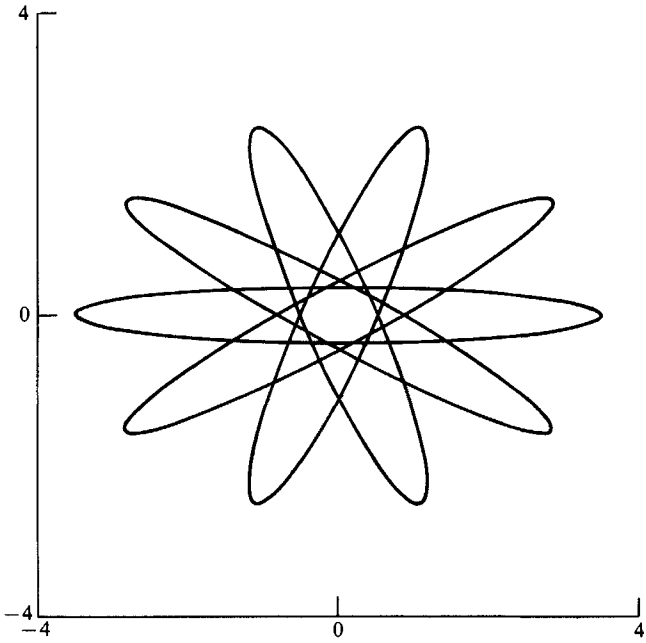

FIGURE 2. Plot of the elliptical cross-section of the torus on which the torus knot is wrapped as a function of time. Parameter values are $|\kappa_+| = 2.0$, $|\kappa_-| = 1.4$, $\mu = 3/2$ (a trefoil knot).

pictures. We know that the torus knot is wrapped on an elliptical torus, and it is easy to show that the coordinates of the ellipse are given by

$$\left.\begin{aligned} \alpha(x) &= -\frac{2\epsilon}{\gamma^2}(|\kappa_+|\cos(\mu x+\phi_+)+|\kappa_-|\cos(\mu x+\phi_-)),\\ \beta(x) &= -\frac{2\epsilon}{\gamma\mu}(|\kappa_-|\sin(\mu x+\phi_-)-|\kappa_+|\sin(\mu x+\phi_+)). \end{aligned}\right\} \tag{5.15}$$

In figure 2 we show the ellipses (5.15) (the cross-section of the torus) with parameter values $|\kappa_+| = 2.0$, $|\kappa_-| = 1.5$, $\mu = 3/2$ (a trefoil knot), and $\epsilon = \frac{1}{2}\gamma$ for a sequence of five values of $\phi_+ - \phi_-$. From this sequence of plots, we see that the torus on which the knots are wrapped has a cross-section that is a rotating ellipse that is also changing its shape as it rotates as a function of time.

The third aspect of the motion of this curve is that it 'slides' on the surface of the deforming torus. The sliding motion is easiest to visualize by recalling that $\beta(x)$ in (5.15) is the vertical component of the curve and x is proportional to the angular variable of the large circle of the underlying torus. Thus, $\beta(x)$ represents projection of the torus onto a cylinder. Clearly, the function $\beta(x)$ is the superposition of two travelling waves, moving in opposite directions, and this reflects the way in which the knot slides along the torus. Of course, if the amplitudes of these two waves are quite different, then the curve would appear as one large-amplitude wave moving in one direction with a smaller wave sitting on top of the first, moving in the opposite direction.

The full motion of the knot consists of sliding the curve on a torus whose large radius is breathing and whose elliptical cross-section is rotating and periodically varying as illustrated by figure 2. Finally, the form of the solution suggests that it

is quasi-periodic with two basic, but incommensurate, temporal periods (Tracy & Chen 1988). Indeed, the two-soliton solution of the nonlinear Schrödinger equation to which this solution corresponds is a quasi-periodic period with two basic periods. Of course, as higher modes are added to the solution to accommodate general initial data, the number of incommensurate periods increases, so that the general solution is at best almost periodic. For small ϵ, however, these perturbations do not change the topology of the torus knot.

6. Cable knots

Torus knots are the simplest knots that can be constructed as small perturbations from circular solutions. In the previous section we constructed a torus knot by wrapping a curve on a torus that has been expanded from a central circular filament. However, we could have started with any closed curve as the central filament for the torus, and wrapped a torus knot on that expanded torus. That is, we could wrap a torus knot onto a torus that has as its central filament another knotted curve. In this way we construct the so-called cable knots, or iterated torus knots. Of course, the process can be repeated as often as desired. We start with a circular central filament, expand it to a torus and then wrap a torus knot onto it. We then take the resulting knotted curve, expand it into a torus, and wrap another torus knot onto it, and so on. Thus a cabled knot can be viewed as resulting from a cascading iteration of torus knot bifurcations (Crawford & Omohundro 1984).

To classify the cabled knots, we keep track of the winding number on each of the tori. That is, we have a sequence of winding numbers m_1/n_1, m_2/n_2, ..., m_k/n_k, describing the torus knot used at each level of the cascade. For 'small-amplitude' cable knots, we need to determine how the curvature and torsion oscillate as the angular variable for the underlying circle is traversed. We know, for example, that for a small-amplitude m_1/n_1 torus knot, the curvature and torsion oscillate sinusoidally m_1 times as the underlying circle is traversed n_1 times. To create a new m_2/n_2 torus knot on the first m_1/n_1 torus knot, the curvature and torsion must oscillate m_2 times as the length of the first torus is traversed n_2 times. That is, the curvature and torsion must oscillate m_2 times as the original underlying circle is traversed $n_1 n_2$ times. Therefore, to create cable knots with the sequence of winding numbers m_1/n_1, m_2/n_2, ..., m_k/n_k, we look for curvature and torsion with oscillatory components having relative frequencies in the ratio

$$1 : \frac{m_1}{n_1} : \frac{m_2}{n_1 n_2} : \frac{m_3}{n_1 n_2 n_3} : \ldots : \frac{m_k}{n_1 n_2 \ldots n_k}. \tag{6.1}$$

As a specific example, a trefoil knot wrapped on a trefoil knotted torus would have curvatures with relative frequencies $1 : \frac{3}{2} : \frac{3}{4}$. In figure 3(*a*) is shown a trefoil cabling (solid curve) of a trefoil knot (dashed curve). In figure 3(*b*) is shown a 5/2 cabling of a 5/2 torus knot.

We wish to explore the dynamic behaviour of small-amplitude cabled knots for the equations of motion $\boldsymbol{R}_t = \kappa \boldsymbol{B}$. This is equivalent to studying the behaviour of (4.1) with many spatially oscillatory modes of comparable amplitude. For this discussion we shall limit our investigation to the simplest possible cabling that gives interesting results, namely, an m/n torus knot with an $m/2$ cabling. The corresponding curvature and torsion oscillate with relative frequencies m/n for the torus knot, and $m/2n$ for the cabling. The reason this cabling is mathematically interesting is because the two oscillations are nonlinearly resonant at the lowest possible order. Other

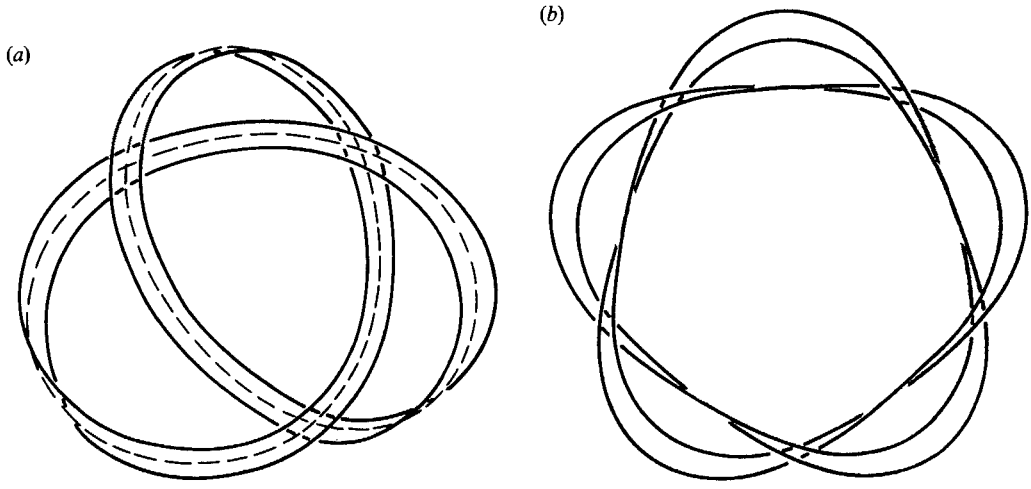

FIGURE 3. (*a*) A trefoil cabling (solid curve) of a trefoil knot (dashed curve), and (*b*) a 5/2 cabling of a 5/2 knot.

cablings produce resonances at a higher order and therefore require calculation of higher-order terms before interesting nonlinear effects are uncovered.

The procedure is identical to that in the previous section, except that now the form of the assumed solution has more leading-order contributions, being of the form

$$\left.\begin{aligned}\kappa(x,t,\epsilon) &= \kappa_0(t,\epsilon)+\sum_{j=1}^{\infty}\epsilon^j(\kappa_{2j-1}(t,\epsilon)\,e^{i(2j-1)\mu x}+\kappa_{2j}(t,\epsilon)\,e^{2ij\mu x}+\text{c.c.}),\\ \tau(x,t,\epsilon) &= \tau_0(\epsilon)+\sum_{j=0}^{\infty}\epsilon^j(\tau_{2j-1}(t,\epsilon)\,e^{i(2j-1)\mu x}+\tau_{2j}(t,\epsilon)\,e^{2ij\mu x}+\text{c.c.}),\end{aligned}\right\} \tag{6.2}$$

where by c.c. we mean the complex conjugate of the previous expression, and $\mu/\kappa_0 = m/2n$. With the solution expressed in the form (6.1), the components κ_2 and τ_2 correspond to the first torus knot and the components κ_1 and τ_1 correspond to its cabling.

We once again use the method of harmonic balance to expand the system of equations (4.1) into a hierarchy of differential equations governing the behaviour of the amplitude of each of the modes $e^{ij\mu x}$. To include the $O(\epsilon^2)$-effects, we must keep equations for the modes zero to 4 of (6.2). Because they are rather complicated, we do not display these equations here, although they are similar in form to (5.2), (5.3), (5.4), but with more terms.

The leading-order equations are not so complicated. They are

$$\left.\begin{aligned}\frac{d\kappa_1}{dt} &= -i\mu\kappa_0\tau_1, & \frac{d\tau_1}{dt} &= i\mu(\kappa_0^2-\mu^2)\frac{\kappa_1}{\kappa_0},\\ \frac{d\kappa_2}{dt} &= -2i\mu\kappa_0\tau_2, & \frac{d\tau_2}{dt} &= 2i\mu(\kappa_0^2-4\mu^2)\frac{\kappa_2}{\kappa_0},\end{aligned}\right\} \tag{6.3}$$

and their general solutions are

$$\left.\begin{aligned}\kappa_1(t) &= \kappa_{1-}e^{-i\omega_1 t}+\kappa_{1+}e^{i\omega_1 t}, & \tau_1(t) &= \frac{\omega_1}{\mu\kappa_0}(\kappa_{1-}e^{-i\omega_1 t}-\kappa_{1+}e^{i\omega_1 t}),\\ \kappa_2(t) &= \kappa_{2-}e^{-i\omega_2 t}+\kappa_{2+}e^{i\omega_2 t}, & \tau_2(t) &= \frac{\omega_2}{2\mu\kappa_0}(\kappa_{2-}e^{-i\omega_2 t}-\kappa_{2+}e^{i\omega_2 t}),\end{aligned}\right\} \tag{6.4}$$

where $$\omega_1^2 = \mu^2(\mu^2-\kappa_0^2), \quad \omega_2^2 = 4\mu^2(4\mu^2-\kappa_0^2).$$

For these solutions to be bounded, we must require $\mu > k_0$. Since $\mu/\kappa_0 = m/2n$, the ensuing analysis does not apply to the cabling of a trefoil knot, for which $m/2n = 3/4 < 1$. The simplest knot for which this analysis applies is the cabling of a 5/2 knot.

Now we use the solutions (6.3) as the leading-order terms of a power series expansion of the solution, assuming as well that the coefficients κ_{1-}, κ_{1+}, κ_{2-}, κ_{2+}, are functions of the slow time-like variable $\sigma = \epsilon^2 t$. We expand the equations of motion into powers of ϵ, taking into account the chain rule (5.7), and proceed to solve this hierarchy of equations, requiring that at each order of ϵ, the solution is a bounded, quasi-periodic function of t. We first find the order-ϵ correction to the leading-order solution (5.6), and then to obtain a bounded, quasi-periodic order-ϵ^2 correction it is necessary to impose conditions on the slow evolution of the functions κ_{1-}, κ_{1+}, κ_{2-}, κ_{2+}. These are

$$\frac{\partial \kappa_{j\pm}}{\partial \sigma} \pm i\Omega_j(|\kappa_{1\pm}|, |\kappa_{1\mp}|, |\kappa_{2\pm}|, |\kappa_{2\mp}|)\,\kappa_{j\pm} = 0 \quad (j = 1, 2), \tag{6.5}$$

where

$$\begin{aligned}
\kappa_0^2 \omega_1 \omega_2 \Omega_1(w, x, y, z) &= \omega_2 p_1(\mu) w^2 - \omega_2 p_2(\mu) x^2 \\
&\quad + (\omega_2 p_3(\mu) - \omega_1 p_4(\mu)) y^2 + (\omega_2 p_3(\mu) + \omega_1 p_4(\mu)) z^2, \\
\kappa_0^2 \omega_1 \omega_2 \Omega_2(w, x, y, z) &= \omega_1 p_1(2\mu) y^2 - \omega_1 p_2(2\mu) z^2 \\
&\quad + (2\omega_1 \omega_2^2 + 8\omega_2 \mu^2 \kappa_0^2) w^2 + (2\omega_1 \omega_2^2 - 8\omega_2 \mu^2 \kappa_0^2) x^2,
\end{aligned}$$

$p_1(\mu)$ and $p_2(\mu)$ are defined in (5.9), and

$$p_3(\mu) = \tfrac{1}{2}(8\mu^4 - 9\mu^2 \kappa_0^2 + \kappa_0^4), \quad p_4(\mu) = 16\mu^4 - 3\kappa_0^4.$$

The solutions of (6.5) are given by

$$\kappa_j = |\kappa_j(0)|\, e^{i\Omega_j \sigma} \quad (j = 1-, 1+, 2-, 2+), \tag{6.6}$$

with the constants Ω_j dependent on the constants $|\kappa_{1\pm}(0)|$ and $|\kappa_{2\pm}(0)|$. Clearly the functions $|\kappa_{1\pm}(\sigma)|$ and $|\kappa_{2\pm}(\sigma)|$ are constants independent of time. The nonlinear interaction is evidenced through the complex phases Ω_j.

With the solution expressed in the form of (6.1) it is necessary to determine when the corresponding solution curve is closed. For this we must recompute the lengthscale $A(\epsilon)$ and the average torsion, using the procedure of §3. The results of this computation are that

$$A(\epsilon) = 1 + \frac{\epsilon^2}{\kappa_0^2}(|\kappa_{1+}|^2 + |\kappa_{1-}|^2 + |\kappa_{2+}|^2 + |\kappa_{2-}|^2) + O(\epsilon^4),$$

$$\tau_0(\epsilon) = \frac{2\mu\epsilon^2}{\omega_1}(|\kappa_{1+}|^2 - |\kappa_{1-}|^2) + \frac{4\mu\epsilon^2}{\omega_2}(|\kappa_{2+}|^2 - |\kappa_{2-}|^2) + O(\epsilon^4),$$

both of which are constant, as expected.

The motion of the iterated torus knot can now be described in terms of three components of its motion. First of all, the underlying circle 'breathes', as the average value of the curvature is given by

$$\begin{aligned}
\kappa_0(t) = \kappa_0 - \frac{\epsilon^2}{\kappa_0}(&\kappa_{1+}(\sigma)\kappa_{1-}^*(\sigma) e^{2i\omega_1 t} + \kappa_{1-}(\sigma)\kappa_{1+}^*(\sigma) e^{-2i\omega_1 t} \\
&+ \kappa_{2+}(\sigma)\kappa_{2-}^*(\sigma) e^{2i\omega_2 t} + \kappa_{2-}(\sigma)\kappa_{2+}^*(\sigma) e^{2i\omega_2 t}).
\end{aligned}$$

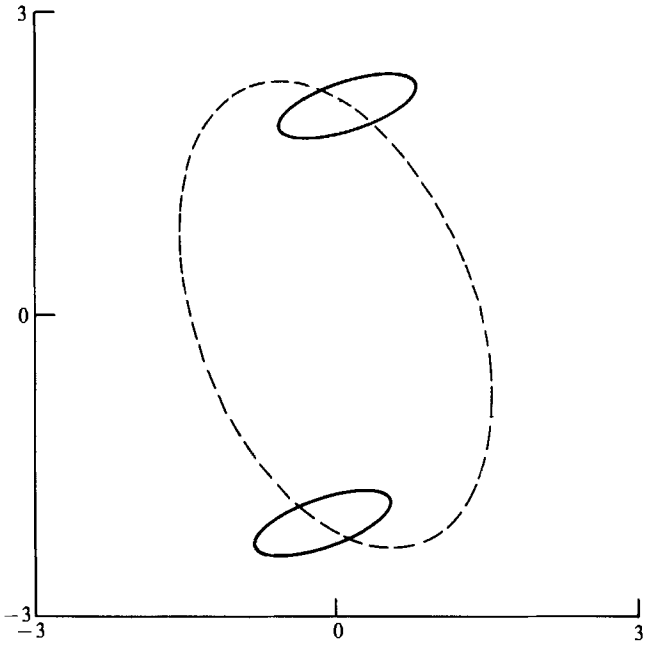

FIGURE 4. Cross-section of the ellipses on which a 5/2 cabling of a 5/2 torus is wrapped. The small ellipses rotate as a function of time around points on the large (dashed) ellipse, which also rotates as a function of time.

Second, the curve is wrapped on in iterated torus, the cross-sections of which are rotating ellipses. For example, if the amplitudes of the second mode $|\kappa_{2\pm}(0)|$, are sufficiently larger than the amplitudes of the first mode $|\kappa_{1\pm}(0)|$, then the curve is wrapped around a small rotating ellipse, which has as its centre a larger rotating ellipse. An example of this configuration is shown in figure 4 where the solid ellipses correspond to taking $|\kappa_{1+}(0)| = 0.6$, $|\kappa_{1-}(0)| = 0.3$, and the large (dashed) ellipse corresponds to $|\kappa_{2+}(0)| = 2$, $|\kappa_{2-}(0)| = 1.5$. For this plot, $2\mu/\kappa_0 = 5/2$, corresponding to a 5/2 cabling of a 5/2 knot. If, on the other hand, the amplitudes $|\kappa_{2\pm}(0)|$ are much smaller than $|\kappa_{1\pm}(0)|$, then the knot is a simple torus knot with winding number $\mu = m/2n$. This is because a torus knot is perturbed by a smaller amplitude oscillation with relative frequencies of oscillation $m/2n : m/n$. Because of (6.1), this corresponds to a $2m/1$ cabling of an $m/2n$ torus knot, which is merely a perturbation of the original torus knot that does not change its topology.

The third component of the motion is a superposition of four travelling waves sliding along the underlying torus structure. The full motion is quasi-periodic with four basic periods, as is known from the four soliton solution of the nonlinear Schrödinger equation. However, higher-order modes will in general add small-amplitude components with additional incommensurate periods, leading to an almost periodic motion. For small ϵ, however, the topology of the knot will not be changed by higher-order corrections.

The topology of the cabled knot is not always invariant. In the case suggested by figure 4, the topology is invariant if the two smaller ellipses never intersect as they rotate and move around the rotating larger (dashed) ellipse. However, if the amplitudes of the modes are not sufficiently disparate, so that the two smaller ellipses do intersect at some time, then the knotted curve may have self-intersections and

pass through itself to change the topology of the knot. When the ellipses separate, the original topology of the knot must be restored. The topology of the perturbed (but not cabled) torus knot is invariant as a function of time.

The behaviour of these solutions when there are self-intersections and changes of topology cannot be correct for vortex motions of a real fluid. The equations solved here include no non-local effects, so the solutions do not feel the influence of self-intersections of different parts of the same curve.

7. Discussion

Using perturbation arguments we have determined the behaviour of knotted solutions of the equation of self-induced motion of a vortex in an ideal fluid. Since these solutions are found by perturbation arguments, they are 'small-amplitude' knots, that is, the small radius of the torus about which they are wrapped is of small amplitude compared to the large radius of the torus. The structure of these knotted solutions for larger amplitudes must be studied numerically, or using a fully nonlinear method based on the solvability of the nonlinear Schrödinger equation. The difficulty with large-amplitude solutions is finding closed solutions of the Frenet–Serret equations and determining their topology. Since the motion of the filament is governed solely by local features of the filament, there is no way to guarantee that at larger amplitudes the filaments do not intersect and change their topological structure. The fact that the equations of motion include no non-local effects is a weakness of the theory.

We have demonstrated this solution technique for the equation of self-induced motion of a vortex filament in an ideal fluid, but the technique of finding small-amplitude torus knots is quite general, and knots are easily found as structures which bifurcate from rotating invariant circles. This technique has been applied to find twisted and knotted scroll rings in excitable media (Keener 1989). The success of the method depends entirely on the nature of the normal and binormal velocities α and β, which are determined by the physics of a particular problem. If, for a particular choice of α and β, there is, first of all, an invariant circle, and secondly, a linearized equation that has periodic curvatures and torsions, then standard perturbation arguments yield the torus knots.

Much of the literature on knots deals with their topological features rather than with differential equations that may have knotted solutions. Previous studies of knots in physical contexts have examined solutions of the Euler elastica in three dimensions (Langer & Singer 1984) and the strength of knotted ropes (Maddocks & Keller 1987).

The method presented here finds only torus and iterated torus knots, because there is an obvious description of these knots through bifurcation of period-multiplying orbits. Another context in which knots play a role is in the study of trajectories of autonomous differential equations in $\mathbb{R}^3$ (Birman & Williams 1983*a*, *b*; Crawford & Omohundro 1984; Hockett & Holmes 1987; Holmes & Williams 1985; Holmes 1987). If a differential equation in $\mathbb{R}^3$ has a periodic orbit, then a bifurcation from this periodic orbit to another periodic orbit of higher periodicity may have a knotted trajectory. If the eigenvalues of the return map (defined in a neighbourhood of the periodic orbit) pass through the unit circle, we knot that there is a bifurcation to a flow on an invariant torus. If the flow on this torus has a closed orbit, it is a knot whenever the rotation number for the flow on the torus is non-integer and bigger than one (Crawford & Omohundro 1984). In this work, bifurcation of knots was the

mechanism that allowed us to construct solutions of our equation, but this does not mean that one should expect to see actual vortex filaments bifurcate from one type of closed curve to another as some parameter of the flow is changed.

The topological structure of vortex motion is certainly of interest in the study of fluid motion (Moffatt 1969, 1985). However, care must be exercised in trying to conclude something from this work about the motion of real fluids. First, the self-induction hypothesis requires that different segments of the filament remain sufficiently separated so that only local effects need to be included. Because we used a perturbation method to write down our knotted solutions, the knotted curves we found are very nearly circular and therefore always in violation of the 'sufficiently separated' assumption. To overcome this difficulty, one could extend these solutions to larger amplitude solutions using numerical techniques or exact methods using hyperelliptic functions, and thereby avoid near self-intersections. Alternatively, one could hope to apply these results to a superfluid in which interactions between different segments of a filament are thought to be important only when the distance between two parts of the same filament is on the order of a few angstroms (Schwarz 1985). A second source of inaccuracy is that the equations solved here do not include other important effects of real fluids, such as finite viscosity, or finite vortex core size. Modifications of the equation of motion to account for these effects have been derived (Callegari & Ting 1978). Since the leading-order behaviour is governed by an equation that is completely integrable and for which the solution can, in principle, be completely specified, it may be possible to study the behaviour of the solutions of the modified equation using a standard perturbation theory for solitons (Keener & McLaughlin 1977; McLaughlin & Scott 1978).

This work was supported in part by NSF grant DMS 8801446. The author is indebted to Professors R. Stern, A. Treibergs, and S. Strogatz for valuable discussions about knots.

Note added in proof. The equations (2.17) show that the integrals of the τ and κ^2 around any closed curve are invariant. From a different (but equivalent) formulation of the equations of torsion and curvature (Betchov 1965; Germano 1983) one can show that the integral of the product $\tau\kappa^2$ around a closed curve is also invariant. Presumably there are an infinite number of such integral invariants.

REFERENCES

Batchelor, G. K. 1967 *An Introduction to Fluid Dynamics*. Cambridge University Press.

Betchov, R. 1965 On the curvature and torsion of an isolated vortex filament. *J. Fluid Mech.* **22**, 471–479.

Birman, J. S. & Williams, R. F. 1983*a* Knotted periodic orbits in dynamical systems I: Lorenz's equations. *Topol.* **22**, 47–82.

Birman, J. S. & Williams, R. F. 1983*b* Knotted periodic orbits in dynamical systems II: Knot holders for fibered knots. *Contemp. Maths* **20**, 1–60.

Callegari, A. J. & Ting, L. 1978 Motion of a curved vortex filament with decaying vortical core and axial velocity. *SIAM J. Appl. Maths* **35**, 148–175.

Chow, S. N. & Hale, J. K. 1982 *Methods of Bifurcation Theory*. Springer.

Cole, J. D. 1968 *Perturbation Methods in Applied Mathematics*. Waltham, Ma: Blaisdel.

Crawford, J. D. & Omohundro, S. 1984 On the global structure of period doubling flows. *Physica* D **13**, 161–180.

GERMANO, M. 1983 On the rediscovery of the DaRios intrinsic equations describing the evolution of a filament vortex. *Alti VII Congresso Nazionale AIDAA*, Vol. 1, pp. 163–170.

HASIMOTO, H. 1972 A soliton on a vortex filament. *J. Fluid Mech.* **51**, 477–485.

HOCKETT, K. & HOLMES, P. 1987 Nonlinear oscillators, iterated maps, symbolic dynamics, and knotted orbits. *Proc. IEEE* **75**, 1071–1079.

HOLMES, P. J. 1987 Knotted periodic orbits in suspensions of annulus maps. *Proc. R. Soc. Lond.* A **411**, 351–378.

HOLMES, P. J. & WILLIAMS, R. F. 1985 Knotted periodic orbits in suspensions of Smale's horseshoe: Torus knots and bifurcation sequences. *Arch. Rat. Mech. Anal.* **90**, 115–194.

KEENER, J. P. 1988*a* The dynamics of three dimensional scroll waves in excitable media. *Physica* D **31**, 269–276.

KEENER, J. P. 1988*b* *Principles of Applied Mathematics: Transformaton and Approximation.* Addison-Wesley.

KEENER, J. P. 1989 Knotted scroll wave filaments in excitable media. *Physica* D **34**, 378–390.

KEENER, J. P. & MCLAUGHLIN, D. W. 1977 Solitons under perturbation. *Phys. Rev.* A **16**, 777–790.

KEENER, J. P. & TYSON, J. J. 1988 The motion of untwisted untorted scroll waves in Belousov–Zhabotinsky reagent. *Science* **239**, 1284–1286.

KIDA, S. 1981 A vortex moving without change of form. *J. Fluid Mech.* **112**, 397–409.

KIDA, S. 1982 Stability of a steady vortex filament. *J. Phys. Soc. Japan* **51**, 1655–1662.

LAMB, G. L. 1981 *Elements of Soliton Theory.* Wiley-Interscience.

LANGER, J. & SINGER, D. A. 1984 Knotted elastic curves in $\mathbb{R}^3$. *J. Lond. Math. Soc.* **30**, 512–520.

MADDOCKS, J. H. & KELLER, J. B. 1987 Ropes in equilibrium. *SIAM J. Appl. Maths* **47**, 1185–1200.

MASSEY, W. S. 1967 *Algebraic Topology: An Introduction.* Harcourt, Brace and World.

MCLAUGHLIN, D. W. & SCOTT, A. C. 1978 A multisoliton perturbation theory. In *Solitons in Action* (ed. Lonngren and Scott), Academic.

MOFFAT, H. K. 1969 The degree of knottedness of tangled vortex lines. *J. Fluid Mech.* **35**, 117–120.

MOFFAT, H. K. 1985 Magnetostatic equilibria and analogous Euler flows of arbitrarily complex topology. Part 1. Fundamentals. *J. Fluid Mech.* **159**, 359–378.

SCHWARZ, K. W. 1985 Three-dimensional vortex dynamics in superfluid ^{4}He: Line–line and line–boundary interactions. *Phys. Rev.* B **31**, 5782–5803.

SCHWARZ, K. W. 1988 Three-dimensional vortex dynamics in superfluid ^{4}He: Homogeneous superfluid turbulence. *Phys. Rev.* B **38**, 2398–2417.

STOKER, J. J. 1966 *Nonlinear Vibrations.* Wiley-Interscience.

STOKER, J. J. 1969 *Differential Geometry.* Wiley-Interscience.

TRACY, E. R. & CHEN, H. H. 1988 Nonlinear self-modulation: An exactly solvable model. *Phys. Rev.* A **37**, 815–839.